Supplementary Information for Anomalous behavior of the Ni^{1+} moment in bi-infinite-layered $La_3Ni_2O_5F$

Young-Joon Song[1,2], Warren E. Pickett[3], and Kwan-Woo Lee[4,5]
[1] *Institut für Theoretische Physik, Goethe-Universität Frankfurt, Max-von-Laue-Straße 1, 60438 Frankfurt am Main, Germany*
[2] *Asia Pacific Center for Theoretical Physics, Pohang, 37673, Korea*
[3] *Department of Physics and Astronomy, University of California, Davis, California 95616, USA*
[4] *Division of Semiconductor Physics, Korea University, Sejong 30019, Korea*
[5] *Department of Applied Physics, Graduate School, Korea University, Sejong 30019, Korea*
(Dated: September 20, 2026)

In this Supplementary Information, we present the additional results obtained from WIEN2K [1], unless mentioned otherwise.

S1. NONMAGNETIC RESULTS

The nonmagnetic (NM) band structure within the the generalized gradient approximation (GGA) exchange-correlation (XC) functional [2] is displayed in Fig. S1. For the $pd\sigma$ bands in the 2D bi-layered square lattice, the 2×2 Hamiltonian can be described by

$$\hat{H}(\boldsymbol{k}) = \begin{pmatrix} \epsilon(\boldsymbol{k}) & T_\perp(\boldsymbol{k}) \\ T_\perp((k) & \epsilon(\boldsymbol{k}) \end{pmatrix}, \tag{1}$$

where the intralayer interaction is

$$\epsilon(\boldsymbol{k}) = \varepsilon_d + 2t_{100}\big[\cos(k_x a) + \cos(k_y a)\big] + 4t_{110}\cos(k_x a)\cos(k_y a) \tag{2}$$

with the on-site energy ε_d relative to E_F, and the interlayer interaction is

$$T_\perp(\boldsymbol{k}) = t_\perp + 4t'_{\perp,110}\cos(k_x a)\cos(k_y a), \tag{3}$$

neglecting a tiny t_{101}. The index "101" indicates an interaction of (Ni) atoms in the x-direction (first digit), but between layers in the bilayer (third digit), its value is negligible. $2t_\perp$ is the mean separation between even and odd combinations of the layer hoppings. Applying this to the NM band structure yields $\varepsilon_d = 87$ meV relative to E_F, $t_{100} = -363$ meV, $t_{110} = 94$ meV, $t_\perp = 39$ meV, and $t'_{\perp,110} = -9$ meV. From the Hamiltonian, splittings between even-odd $pd\sigma$ bands at symmetry points are approximately $2(t_\perp + 4t'_{\perp,110})$ at Γ (M) (essentially vanishing) and $2(t_\perp - 4t'_{\perp,110})$ at X, giving the even-odd $pd\sigma$ band splitting of 150 meV at the X point.

The fatband plots of the La1/La2 5d and O p orbitals, enlarged in the range –1 eV to 1 eV, are displayed in Fig. S2. Figure S3 provides the corresponding total and atom-projected densities of states (PDOSs). The features are described in the caption, note the gap between the O/X 2p states and the flat even $3d_{z^2}$ bands around −2.3 eV.The split van Hove singularities (vHs) just below E_F are evident. For details, see the captions of these figures.

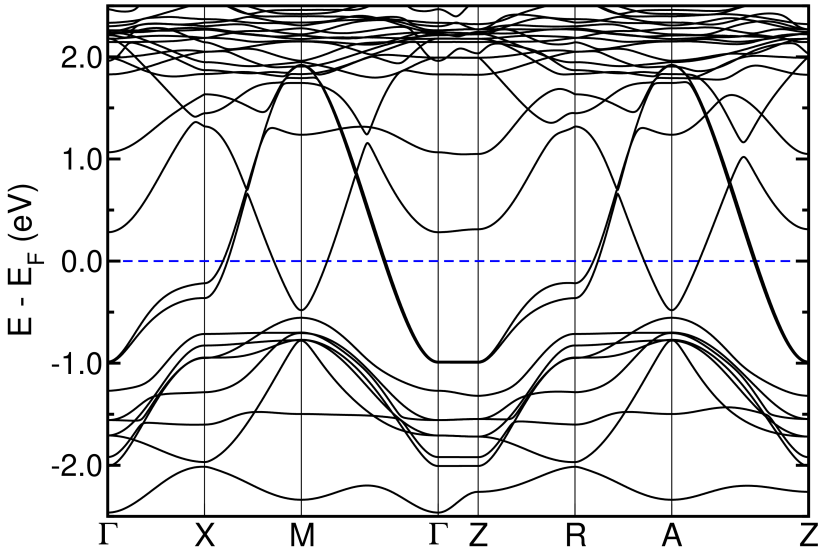


FIG. S1. Band structure for NM $La_3Ni_2O_5F$ with GGA, with a closer look at the behavior of the interstitial E^* band. It dips down from 1.5 eV (at X) and 2 eV (at Γ) to -0.5 eV at M. This band is linear except when approaching symmetry points. The symmetry points follow those in the standard tetragonal Brillouin zone, *e.g* A=($\frac{1}{2}$, $\frac{1}{2}$, $\frac{1}{2}$).

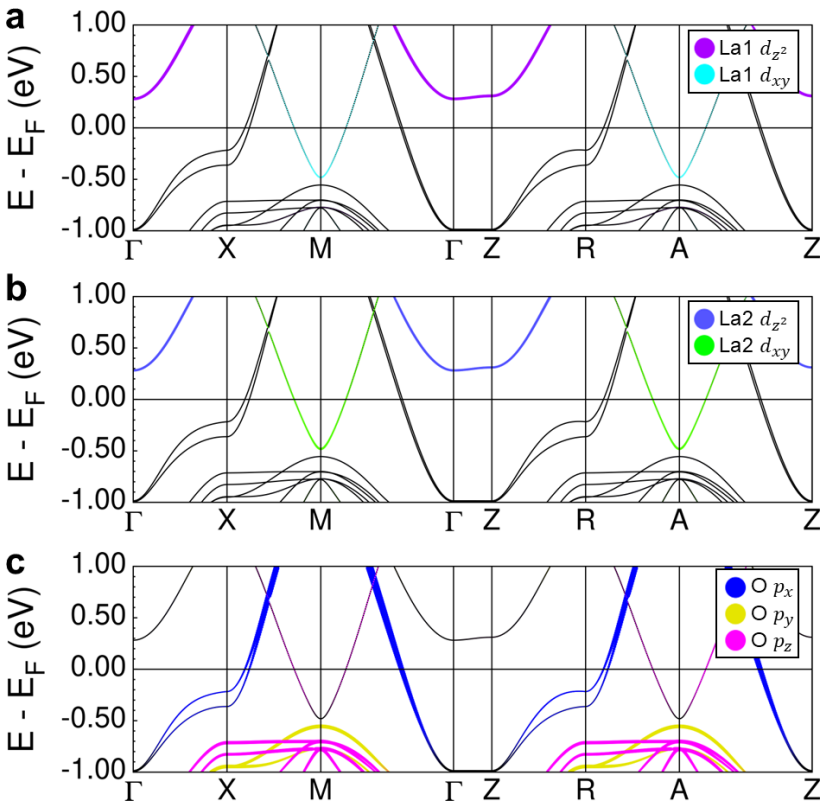


FIG. S2. Corresponding fatband plots of (**a**) La1 5*d*, (**b**) La2 5*d* (similar to La1), and (**c**) O 2*p*, in the range of –1 to 1 eV. The O p_x, p_y, p_z fatbands are for the O atom at $(a/2, 0, 0)$ with respect to the Ni atom, *i.e.* p_x is the p_σ orbital. The La contribution to the E^* band is very small, especially considering its large sphere size, so the two different contributions have been emphasized by a factor of two increase in the line size. The k_z dispersion $\Gamma - Z$ of the $dp\sigma$ band is negligible, no more that 1 meV.

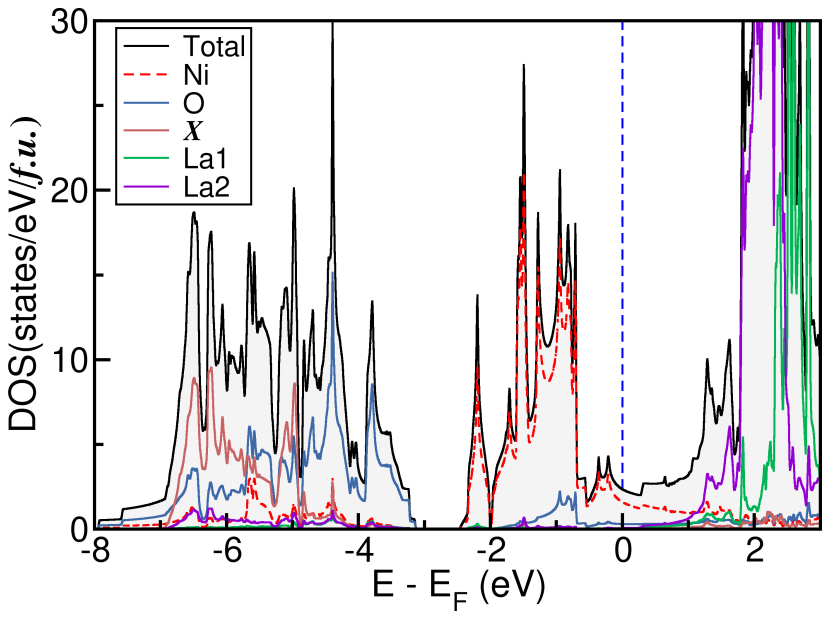


FIG. S3. Total and atom-PDOSs for NM $La_3Ni_2O_5F$ with GGA, showing strong 2D features (jumps in the DOS). Estimating from the centers of each atom-projected DOS, the energy difference of Ni $3d$ and O $2p$ centers is about 4.5 eV, similar to that of $LaNiO_2$. At the Fermi energy E_F the DOS $N(E_F)$ is 2.33 states/eV per f.u., consisting of sphere radii values about 65% Ni d states, 13% O $2p$ states, a minor La contribution and ∼14% interstitial contributions. The values for the $dp\sigma$ and E^* bands, which sum to the total, are given in the main text. The even combination of $3d_{z^2}$ bands lie around −2.3 eV. The $4f$ PDOSs at 2–3 eV indicate that the potential at the La2 site is roughly 0.5 or more lower than on the La1 site. The upper core energies in Table S1 give the more precise value of La2 site energy being 0.43 eV lower than La1.

TABLE S1. This table of core level energies for La1 and La2 may be useful later for a detailed understanding of the $La_3Ni_2O_5F$ electronic structure. Questions may arise also about the (related) difference in $4f$ band positions in Fig S3. The upper core energies of La1 and La2 are very consistent: La2 has a lower site energy than La1 by 0.43 eV. Recall that La2 is part of the blocking layer.

	Core Energy (Ry)		
	La1	La2	ΔE (eV)
1S	-2844.622	-2844.653	0.416
2S	-451.606	-451.638	0.432
2P*	-425.821	-425.852	0.430
2P	-395.455	-395.487	0.431
3S	-95.610	-95.643	0.440
3P*	-84.744	-84.777	0.440
3P	-78.826	-78.858	0.440
3D*	-59.804	-59.836	0.440
3D	-58.538	-58.570	0.440
4S	-18.316	-18.348	0.436
4P*	-14.319	-14.351	0.435
4P	-13.062	-13.094	0.434
4D*	-6.513	-6.545	0.433
4D	-6.295	-6.327	0.433

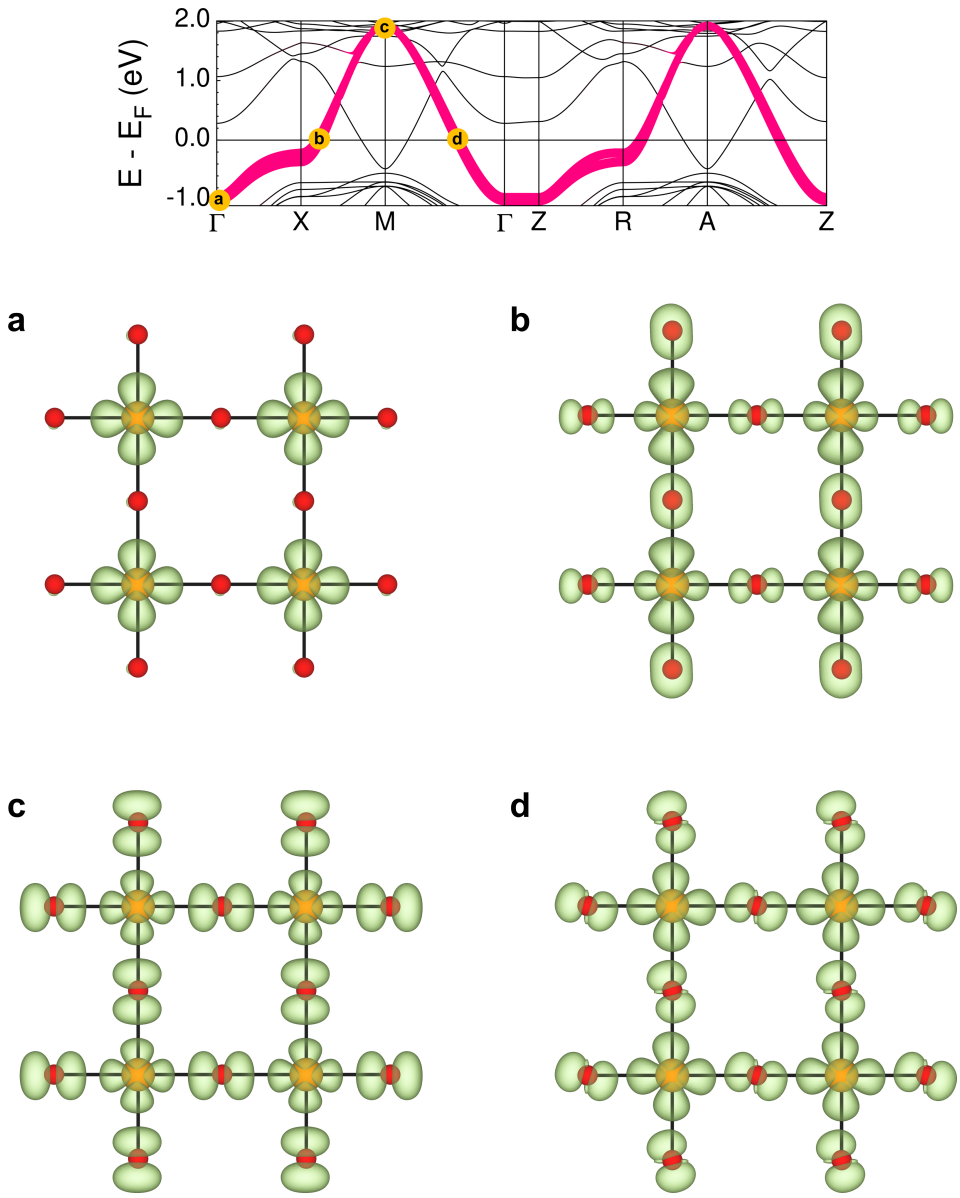


FIG. S4. (Top) $pd\sigma$-projected fatband structure of NM $La_3Ni_2O_5F$ calculated within GGA, with orange markers indicating the $\vec{k}$-points selected for subsequent wavefunction calculations. Panels (**a-d**): Top view of the resulting $pd\sigma$ wavefunction plot $|\Psi(\vec{r})|$ on the NiO_2 layer using the same isovalue. The differences provide an indication of the changing $pd\sigma$ density as energy and $\vec{k}$ are varied throughout the band. Each plot shows (**a**) purely $d_{x^2-y^2}$ or at least nearly so, at Γ, (**b**) $pd\sigma$ bonding, with symmetry of the X-M line, (**c**) $pd\sigma$ M point density with increased p_σ participation and square symmetry, and (**d**) distorted $pd\sigma$ density with symmetry of the M-Γ line.

S2. FIXED SPIN MOMENT STUDIES

In the fixed spin moment (FSM) calculations [3, 4] performed with FPLO [5] using $30 \times 30 \times 30$ k-points in the irreducible zone and the GGA functional [2], the decomposed energy variations are provided in Fig. S5.

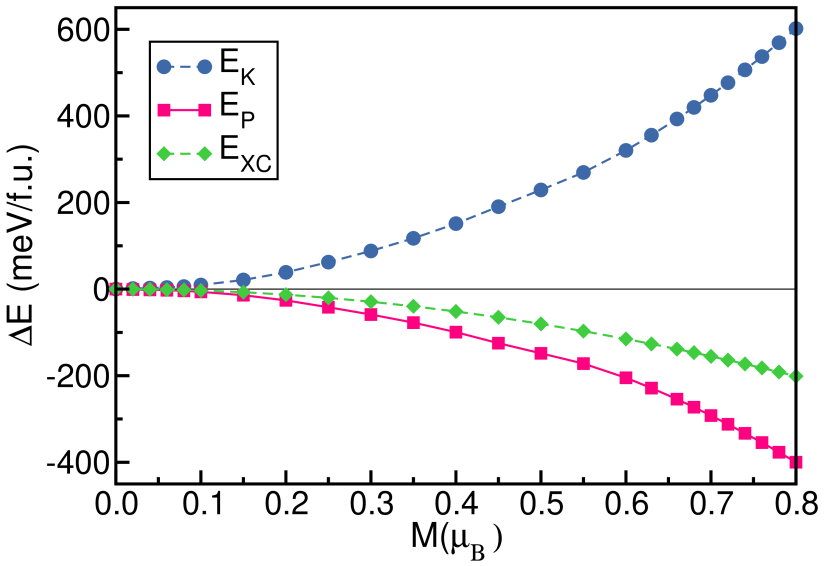


FIG. S5. Decomposed energy variations $\Delta E(M)$ with varying magnitude of the imposed moment M.In this range of M, there is almost perfect cancellation between the magnetic energy gain (sum of E_P and E_{XC}) and the kinetic energy cost (E_K), resulting in only a miniscule increase of no more than 1 meV, see Fig. 3 in the main text. Note that the gain in energy E_P due to the change in density $n(\vec{r}; M)$ is twice that of conventionally pictured gain from direct polarization E_{XC}.

S3. FERROMAGNETIC ALIGNMENT

The band structures of ferromagnetic (FM) $La_3Ni_2O_5F$ within GGA and GGA+U are given in Figs. S6 and S7, respectively. Figure S8 shows the corresponding DOSs.

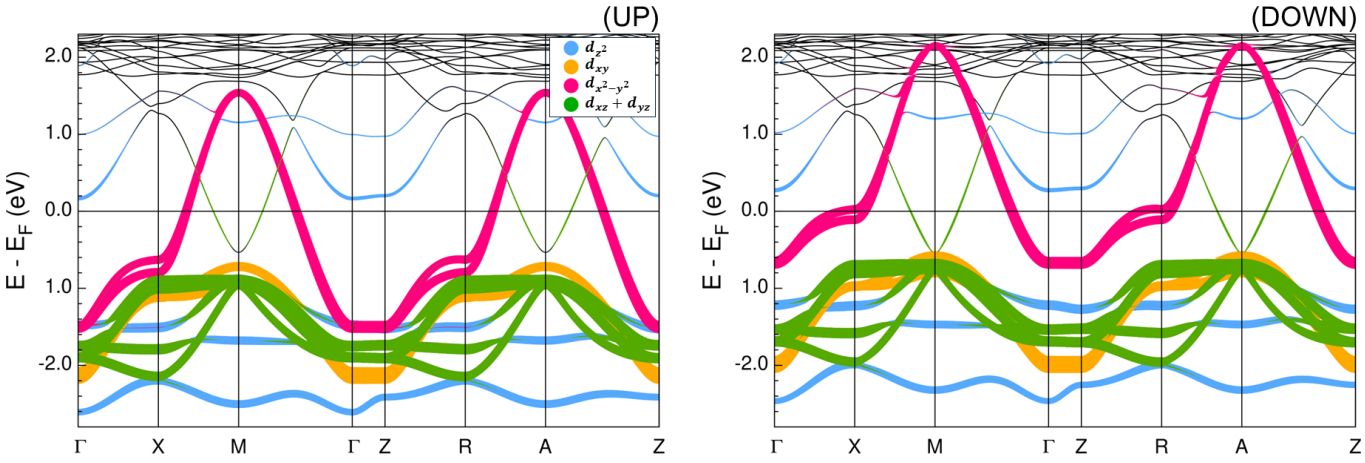


FIG. S6. GGA band structure of FM $La_3Ni_2O_5F$, in the range of –3 to 2 eV, with the spin-up Ni $3d$ fatbands plot on the left, the spin-down on the right. The exchange splitting is about 0.6 eV at X. Both the majority and minority $3d_{x^2-y^2}$ orbitals of Ni are partially filled, leading to a small local moment of 0.34 μ_B/Ni. There are two effects of polarization: a splitting of the $3d_{x^2-y^2}$ bands (typical FM behavior), but the occupied minority bands are narrowed very noticeably. The E^* band filling is unaffected.

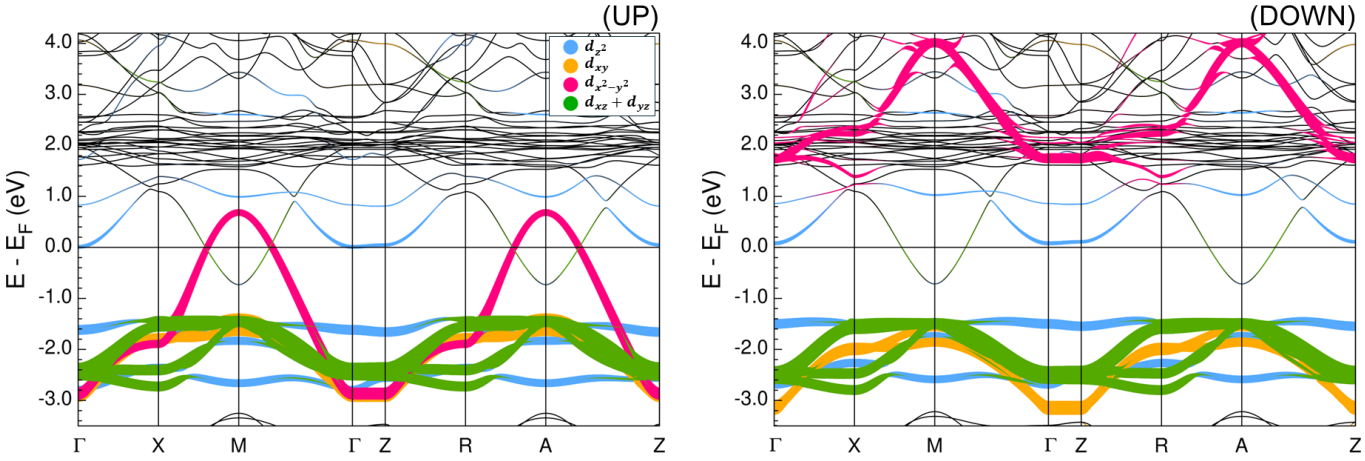


FIG. S7. Band structure (as in the previous figure) of FM $La_3Ni_2O_5F$ within GGA+U ($U_{eff} = 4$ eV) using the AMF double-counting scheme [6], with the overlaid Ni $3d$ fatbands. The unoccupied minority bands are greatly narrowed, with little change in the E^* band filling. The exchange splitting has been increased to ∼4 eV by this value of U_{eff}, however a pocket of $3d$ holes remains equal in density to the E^* electrons, making their circular majority FSs identical. Note: the M-centered electron FS remains unchanged even for U_{eff} up to 5 eV.

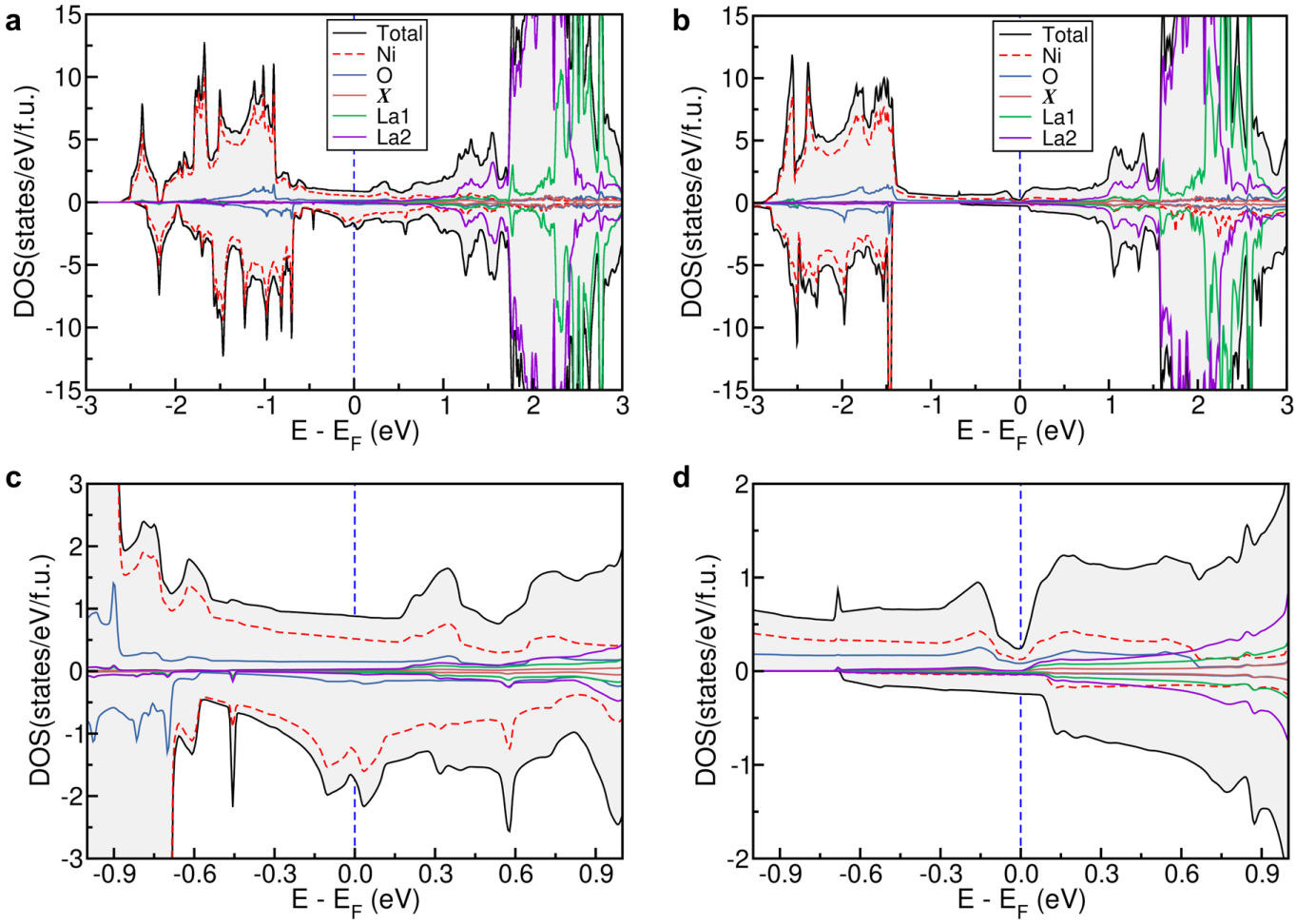


FIG. S8. Total and atom-PDOSs of FM $La_3Ni_2O_5F$ within (**a, c**) GGA and (**b, d**) GGA+U (U_{eff} = 4 eV) using the AMF double-counting scheme [6]. The difference is mainly the additional exchange (Mott) splitting given by U_{eff}, 0.7 eV for GGA, 4.5 eV for GGA+U. These values are measured from the center of up/down $pd\sigma$ bands in the band structures given Figs. S6 and S7. As shown in (**d**), the minority vHs lies 0.3 eV above E_F, while E_F falls between the majority vHs.

S4. ANTIFERROMAGNETIC ALIGNMENT

The GGA band structure of the G-AFM $La_3Ni_2O_5F$ is shown in Fig. S9. Figure S10 shows the fatband plots of La ions ($5d$) and planar O ion ($2p$). The electron (central) and hole (edges) FSs in GGA are described with orbital characters in Fig. S11. Additionally, the atom-projected DOSs within GGA+U at $U_{eff} = 4$ eV a small energy gap of 0.1 eV (not visible) are provided in Fig. S12.

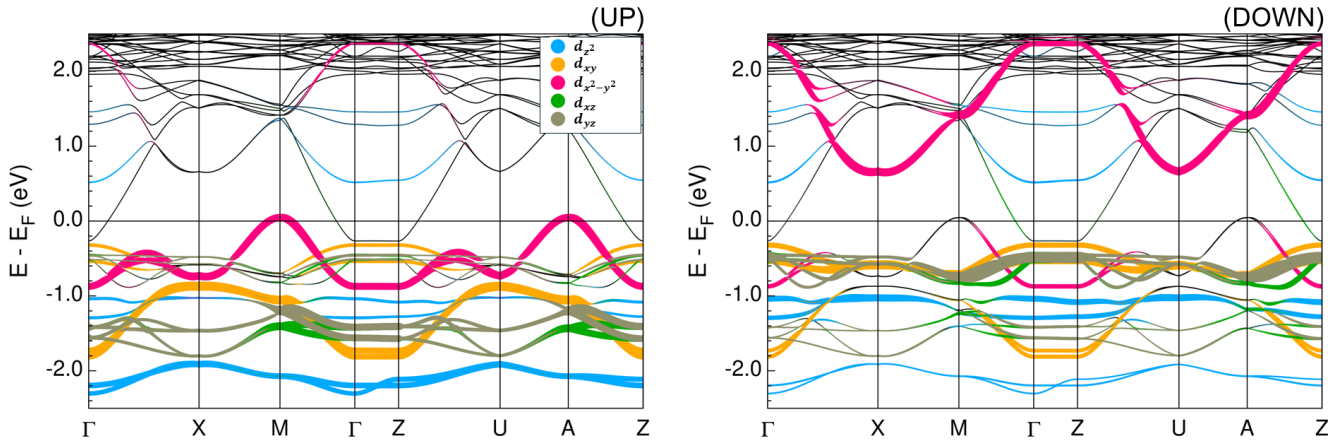


FIG. S9. Band structure of G-AFM $La_3Ni_2O_5F$ within GGA, in the range of –2.5 to 2.5 eV, emphasizing the Ni $3d$ fatband plots for (left) majority and (right) minority characters. Special points are labeled for the AFM Brillouin zone. The filled majority Ni $d_{x^2-y^2}$ band lies below E_F in Mott insulator fashion, while the unfilled minority counterpart is broadened into 0.5 to 2.5 eV range, mixing with upper conduction bands. The exchange splitting of the Ni $3d_{x^2-y^2}$ band centers is ∼2 eV. The E^* band, folded back to Γ, remains with its self-compensating electron carriers and circular FSs for both spin directions.

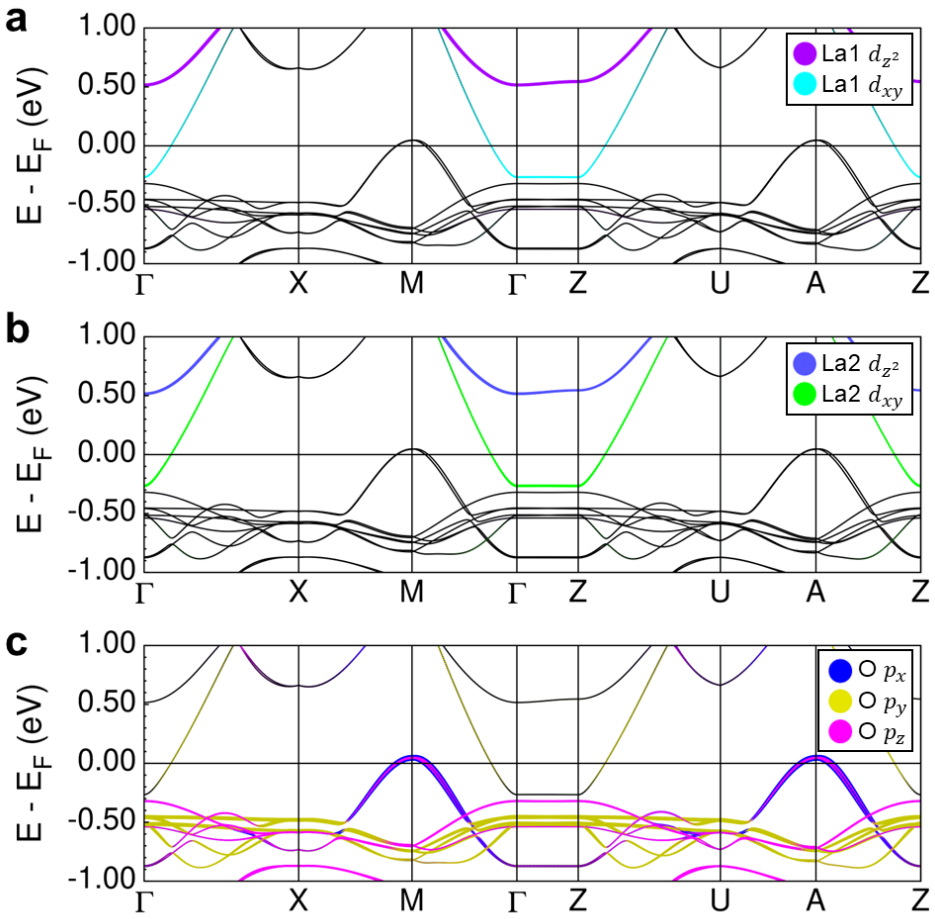


FIG. S10. Fatband plots of (**a**) La1 5*d*, (**b**) La2 5*d*, and (**c**) O 2*p* [O atom at (a/2,0,0) with respect to Ni] for the G-AFM $La_3Ni_2O_5F$ within GGA, enlarged in the range of –1 eV to 1 eV. The "upper Hubbard band" with a small amount of O p_σ character lies above the range of this plot.

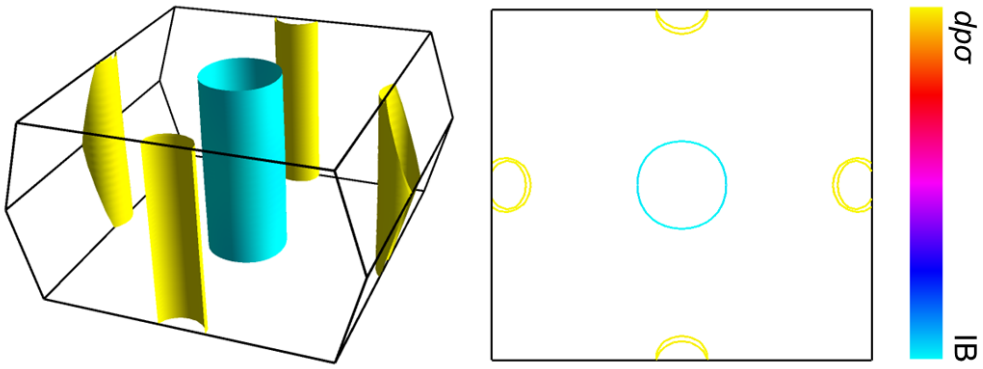


FIG. S11. Fermi surfaces of the G-AFM $La_3Ni_2O_5F$ in GGA, showing extreme 2D character. The Γ-centered tube contains interstitial electrons (folded back from the NM *M* point), while the two *X* centered tubes (along the edges) contain holes, reflecting compensation.

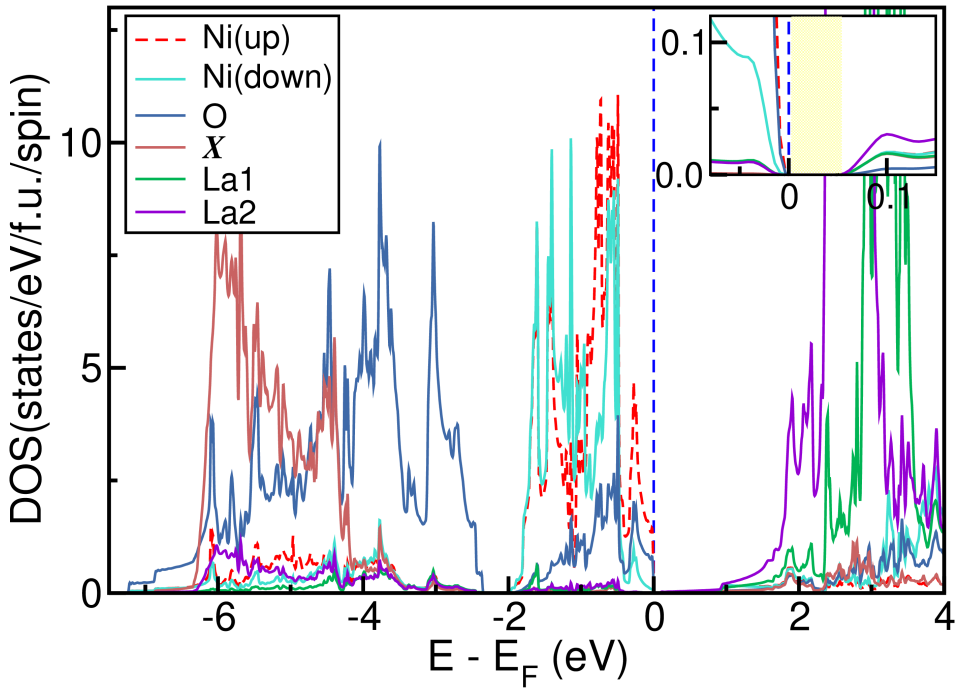


FIG. S12. Atom-PDOSs of the G-AFM $La_3Ni_2O_5F$ within GGA+U ($U_{eff} = 4$ eV), in the full energy range, showing a small energy gap of ∼0.1 eV, visible in the inset. Most Xp orbital character is located in the energy range from −6.2 to −4.2 eV, while the planar O p orbitals span −7.2 to −2.3 eV, mostly in the upper half, in addition to the small but essential p_σ participation in the (primarily minority) $dp\sigma$ band. These O p orbitals are separated from the Ni d orbitals due to crystal field splitting and to $pd\sigma$ hybridization.

[1] P. Blaha, K. Schwarz, F. Tran, R. Laskowski, G. K. H. Madsen, and L. D. Marks, WIEN2k: An APW+lo program for calculating the properties of solids, J. Chem. Phys. Soc. **152**, 074101 (2020).
[2] J. P. Perdew, K. Burke, and M. Ernzerhof, Generalized gradient approximation made simple, Phys. Rev. Lett. **77**, 3865 (1996).
[3] K. Schwarz and P. Mohn, Itinerant metamagnetism in YCo_2, J. Phys. F: Met. Phys. **14**, L129 (1984).
[4] G. L. Krasko, Metamagnetic behavior of fcc iron, Phys. Rev. B **36**, 8565 (1987).
[5] K. Koepernik and H. Eschrig, Full-potential nonorthogonal local-orbital minimum-basis band-structure scheme, Phys. Rev. B **59**, 1743 (1999).
[6] V. I. Anisimov, I. V. Solovyev, M. A. Korotin, M. T. Czyżyk, and G. A. Sawatzky, Density-functional theory and NiO photoemission spectra, Phys. Rev. B **48**, 16929 (1993).